

## Murine intramyocellular lipids quantified by NMR act as metabolic biomarkers in burn trauma

A. ARIA TZIKA<sup>1,2,4</sup>, LOUKAS G. ASTRAKAS<sup>1,2</sup>, HAIHUI CAO<sup>1,2</sup>, DIONYSSIOS MINTZOPOULOS<sup>1,2,4</sup>, QUNHAO ZHANG<sup>1,4</sup>, KATIE PADFIELD<sup>1,4</sup>, HONGUE YU<sup>1,2</sup>, MICHAEL N. MINDRINOS<sup>3</sup>, LAURENCE G. RAHME<sup>4</sup> and RONALD G. TOMPKINS<sup>4</sup>

<sup>1</sup>NMR Surgical Laboratory, Department of Surgery, Massachusetts General Hospital and Shriners Burn Institute, Harvard Medical School, Boston, MA 02114; <sup>2</sup>Athinoula A. Martinos Center of Biomedical Imaging, Department of Radiology, Massachusetts General Hospital, Boston, MA 02114; <sup>3</sup>Department of Biochemistry, Stanford University School of Medicine, Stanford, CA 94305; <sup>4</sup>Department of Surgery, Massachusetts General Hospital and Shriners Burn Institute, Harvard Medical School, Boston, MA 02114, USA

Received February 1, 2008; Accepted March 17, 2008

**Abstract.** It has been suggested that intramyocellular lipids (IMCLs) may serve as biomarkers of insulin resistance and mitochondrial dysfunction. Using a hind-limb mouse model of burn trauma, we tested the hypothesis that severe localized burn trauma involving 5% of the total body surface area causes a local increase in IMCLs in the leg skeletal muscle. We quantified IMCLs from *ex vivo* intact tissue specimens using High-Resolution Magic Angle Spinning (HRMAS) <sup>1</sup>H NMR and characterized the accompanying gene expression patterns in burned versus control skeletal muscle specimens. We also quantified plasma-free fatty acids (FFAs) in burn versus control mice. Our results from HRMAS <sup>1</sup>H NMR measurements indicated that IMCL levels were significantly increased in mice exposed to burn trauma. Furthermore, plasma FFA levels were also significantly increased, and gene expression of Glut4, insulin receptor substrate 1 (IRS1), glycolytic genes, and PGC-1 $\beta$  was downregulated in these mice. Backward stepwise multiple linear regression analysis demonstrated that IMCL levels correlated significantly with FFA levels, which were a significant predictor of IRS1 and PGC-1 $\beta$  gene expression. We conclude from these findings that IMCLs can serve as metabolic biomarkers in burn trauma and that FFAs and IMCLs may signal altered metabolic gene expression. This signaling may result in the observed burn-induced insulin resistance and skeletal muscle mitochondrial dysfunction.

We believe that IMCLs may therefore be useful biomarkers in predicting the therapeutic effectiveness of hypolipidemic agents for patients with severe burns.

### Introduction

Severe burns carry high rates of mortality and morbidity (1,2), and are complicated by the associated development of insulin resistance (3,4) and mitochondrial dysfunction (5). Treatment of patients suffering from burn trauma can also be complicated by organ dysfunction and the late development of infection (1,2). For these reasons, the pathophysiology of burn trauma remains an area of intense study (2). It is believed that early administration of appropriate therapeutic factors may be useful in limiting post-burn metabolic dysfunction. In order to evaluate the effectiveness of such factors, metabolic biomarkers are required.

In addition to its association with burn trauma, insulin resistance is also frequently observed in various metabolic diseases, including obesity, dyslipidemia, arterial hypertension, and type 2 diabetes. Skeletal muscle wasting in insulin-resistant burn patients has been documented and develops due to a lack of anabolic effects, as well as enhanced gluconeogenesis and protein catabolism (6,7) in the burned skeletal tissue. Although the molecular mechanisms underlying abnormal insulin function in burn victims have not been elucidated, there is increasing evidence that plasma-free fatty acids (FFAs) may play a role in inducing insulin resistance (8). Because fatty acid metabolism and glucose levels are closely linked, aberrations in FFA levels, such as through accumulation of lipids or triglycerides in the muscle, may lead to insulin resistance (9).

Aberrations in the peroxisome proliferator-activated receptor coactivator 1 (PPAR $\gamma$  coactivator-1 or PGC-1) family of coactivators (10,11) are also related to metabolic abnormalities. PGC-1 $\alpha$  and PGC-1 $\beta$  are close homologs and share extensive sequence identity (12). In general, PGC-1 coactivators play a critical role in the maintenance of glucose, lipid and energy homeostasis, and are likely to be

---

*Correspondence to:* Dr A. Aria Tzika, NMR Surgical Laboratory, Department of Surgery, Massachusetts General Hospital, Harvard Medical School, Room 261, 51 Blossom Street, Boston, MA 02114, USA

E-mail: atzika@partners.org

**Key words:** nuclear magnetic resonance, skeletal muscle, burn trauma, lipids, PGC-1 $\beta$ , mitochondria, metabolism, biomarkers

involved in pathogenic conditions such as neurodegeneration, cardiomyopathy, obesity, diabetes (13), and potentially, burn injury.

$^1\text{H}$  NMR spectroscopy is a useful method for measuring intramyocellular lipid (IMCL) levels (14,15). The resonances from the methyl and methylene protons of the triglyceride acyl chains appear between 1.0 and 1.6 ppm in the proton NMR spectra. Boesch *et al* and Schick *et al* independently reported that *in vivo* proton NMR spectroscopy detects two sets of resonances from fatty acyl chains within muscle, shifted 0.2 ppm apart (16,17). These investigators suggested that these signals originate from two distinct adipocyte and intramyocellular compartments, which has been further verified by other studies. It has also been suggested that proton NMR spectroscopy may serve as a useful method for monitoring triglyceride levels in adipose or metabolically active muscle cells. Although IMCL levels depend on the muscle type, and the age and gender of the patient (18,19), nevertheless, studies indicate that IMCLs may serve as useful indices of insulin resistance/metabolic abnormality in nondiabetic nonobese humans (20,21). Furthermore, elevated IMCLs have been detected in obese and/or type 2 diabetic patients, where increased IMCL levels are due to impaired insulin-stimulated glucose uptake (22-24).

In addition to NMR spectroscopy, which measures biomarkers in intact systems, the development of high-throughput microarray systems capable of simultaneously measuring the expression of thousands of genes has greatly advanced our ability to detect biomarkers. By exploring the expression of certain organ-specific candidate genes, the biological relevance of NMR data can be validated in experiments examining the same specimen. Combining NMR and microarray data provides an opportunity to cross-validate such data (5).

Here, we measured levels of IMCLs visible by High-Resolution Magic Angle Spinning (HRMAS)  $^1\text{H}$  NMR spectroscopy of intact proximal skeletal muscle tissue samples following burn trauma in mice. We found that increased IMCL levels were a metabolic biomarker for insulin resistance. Furthermore, increased levels of FFAs in the plasma of mice experiencing burn trauma were associated with increased IMCL levels. These results enabled us to propose a molecular mechanism governing burn-induced insulin resistance; plasma FFA levels increase as a result of burn trauma and cause an increase in IMCL levels. This induces insulin resistance through downregulation of the glucose transport system (Glut4) and the insulin receptor substrate 1 (IRS1), where downregulation may occur through the post-transcriptional coactivator PGC-1 $\beta$ .

## Materials and methods

**Experimental animals.** Male, 6-wk-old CD1 mice weighing ~20-25 g were purchased from Charles River Laboratory (Boston, MA). The animals were maintained on a regular light-dark cycle (lights on from 8:00 to 20:00 h) at an ambient temperature of 22 $\pm$ 1 $^\circ\text{C}$ , and had free access to food and water. All animal experiments were approved by the Subcommittee on Research Animal Care of the Massachusetts General Hospital, Boston, MA.

**Hind limb burn model.** Mice were anesthetized by intraperitoneal (i.p.) injection of 40 mg/kg pentobarbital sodium and were randomized into burn or control groups. The left hind limb of all mice in both groups (control and burn) was shaved, and each mouse in the burn group was subjected to a nonlethal scald injury of 3-5% total body surface area (TBSA) by immersion of the left hind limb in 90 $^\circ\text{C}$  water for 3 sec as previously described (25). The total surface area of each mouse was calculated using Meeh's formula:  $A = k \times W^{2/3}$  where A is the surface area in cm $^2$ ; k is the proportionality constant 12.3; and W is the weight in grams. Mice were resuscitated with 2 ml of 0.9% saline i.p. The gastrocnemius muscle was excised from the hind limbs of both control and treated mice, and was immersed in 1 ml TRIzol $^{\text{®}}$  (Gibco BRL, Invitrogen, Carlsbad, CA) for RNA extraction at 6 h, 12 h, 1 day, and 3 days post burn (n=3 measurements at each time point). After injury, the animals were given analgesia in the form of buprenorphine 0.05-0.1 mg/kg SQ, as needed.

**HRMAS  $^1\text{H}$  NMR spectroscopy of skeletal muscle tissue after burn trauma.** Animals were studied with HRMAS  $^1\text{H}$  NMR spectroscopy before and at 6, 24 and 72 h after burn trauma. In burn mice, the skeletal muscle tissue underlying the hind limb burn site was harvested, immediately frozen in liquid nitrogen, and stored at approximately -80 $^\circ\text{C}$ . The muscle tissue at the same site from unburned animals served as controls. Three mice per each category were investigated. HRMAS  $^1\text{H}$  NMR spectroscopy experiments of muscle tissue were performed on a Bruker Bio-Spin Avance NMR spectrometer (proton frequency at 600.13 MHz, 89 mm Vertical Bore) using a 4-mm triple resonance ( $^1\text{H}$ ,  $^{13}\text{C}$ ,  $^2\text{H}$ ) HRMAS probe (Bruker, Billerica, MA). The temperature was maintained at 4 $^\circ\text{C}$  by a BTO-2000 thermocouple unit in combination with a magic angle spinning (MAS) pneumatic unit (Bruker). The MAS speed was stabilized at 4.0 $\pm$ 0.001 kHz by a MAS speed controller. The  $^1\text{H}$  NMR spectra were acquired for all samples using a Carr-Purcell-Meiboom-Gill (CPMG) spin echo pulse sequence,  $[\text{90}^\circ-(\tau-180^\circ-\tau)_n\text{-acquisition}]$ , with an inter-pulse delay ( $\tau$ ) of 250  $\mu\text{sec}$ . Hard 90 $^\circ$  (8  $\mu\text{sec}$ ) and 180 $^\circ$  (16  $\mu\text{sec}$ ) were employed. The relaxation delay was set to 2 sec, and spectra were collected both with and without water suppression. The transverse relaxation time ( $T_2$ ) was measured using the same CPMG pulse sequence by varying n from 0 to 520. Free induction decay (FID) signals were acquired with 8k points, 600 msec acquisition time, 8 dummy scans and 128 scans.

HRMAS  $^1\text{H}$  NMR spectra were analyzed using the MestRe-C NMR software package (Mestrelab Research, Santiago de Compostela, Spain, www.mestrec.com). FIDs were zero-filled to 16k points and apodized with exponential multiplication (1 Hz) before Fourier transformation. The spectra were then manually phased and corrected for baseline broad features (Whittaker smoother, smooth factor 10,000). The Levenberg-Marquardt algorithm was used to least-squares-fit a model of mixed Gaussian/Lorentzian functions to the data.

The  $(\text{CH}_2)_{n-2}$  peak at 1.32 ppm was selected for quantification of IMCL levels. Because the sample was spun at the magic angle, and the sample was much smaller (25  $\mu\text{l}$ ) and more homogeneous (reduced bulk magnetic susceptibility

SPANDIDOSIAN the typical voxel size (1 ml) of *in vivo*  $^1\text{H}$  MRS, PUBLICATIONS cal shift difference was observed between IMCL

and extramyocellular lipids (EMCL). The small size of the muscle biopsies and the fact that the samples were collected from the most myocellular part of the muscle suggest that the main contribution to the  $(\text{CH}_2)_{n-2}$  peak was from IMCLs.

**RNA extraction.** At 6, 24 and 72 h post burn, 3 burn and 3 control mice were anesthetized by i.p. injection of 40 mg/kg pentobarbital, and the gastrocnemius was excised. All mice were then administered a lethal dose of pentobarbital (200 mg/kg i.p.), and the gastrocnemius muscle was immediately immersed in 1 ml TRIzol (Gibco BRL) for RNA isolation. The muscle was homogenized for 60 sec using a Brinkmann Polytron PT 3000 homogenizer (Brinkmann Instruments, Westbury, NY) before extraction of total RNA. Chloroform (200  $\mu\text{l}$ ) was added to the homogenized muscle and mixed by inverting the tube for 15 sec. After centrifugation at 12,000  $\times$  g for 15 min, the upper aqueous phase was collected and precipitated by adding 500  $\mu\text{l}$  isopropanol. Further centrifugation at 12,000  $\times$  g for 10 min separated the RNA pellet, which was then washed with 500  $\mu\text{l}$  70% ethanol and centrifuged at 7,500  $\times$  g for 5 min prior to air-drying. The pellet was resuspended in 100  $\mu\text{l}$  DEPC- $\text{H}_2\text{O}$ . An RNeasy Kit (Qiagen, Valencia, CA) was used to purify the RNA according to the manufacturer's protocol. Purified RNA was quantified by UV absorbance at 260 and 280 nm and stored at  $-70^\circ\text{C}$  for DNA microarray analysis.

**Microarray hybridization.** Biotinylated cRNA was generated with 10  $\mu\text{g}$  of total cellular RNA according to the protocol outlined by Affymetrix Inc. (Santa Clara, CA). cRNA was hybridized onto MOE430A oligonucleotide arrays (Affymetrix), stained, washed, and scanned according to Affymetrix protocol.

**Genomic data analysis.** The scanned images of cRNA hybridization were converted to cell intensity files (.CEL files) with the Microarray suite 5.0 (MAS, Affymetrix). The data were scaled to a target intensity of 500, and for each time point all possible pairwise array comparisons of the replicates to control mice were performed (i.e., four combinations when the two arrays from each time point were compared to the two arrays from control mice), using a MAS 5.0 change call algorithm. Probe sets that had a signal value difference  $>100$  and in which both samples were present were scored as differentially modulated when i) the number of change calls in the same direction were at least 3, 4, and 6 when the number of comparisons were 4, 6, and 9, respectively; and ii) the other comparisons were unchanged. Such scoring was to partially compensate for biological stochasticity and technical variation. Based on the ratios of 100 genes determined to be invariant in most of the conditions tested (Affymetrix) in the hind limb burn and control animals, an additional constraint of a minimum ratio of 1.65 was applied to control the known false positives at 5% hind limb.

**Electron microscopy analysis.** Briefly, hind leg skeletal muscle of the control and burn mice was dissected and fixed in 2% glutaraldehyde in 0.1 M cacodylate buffer overnight at  $4^\circ\text{C}$ .

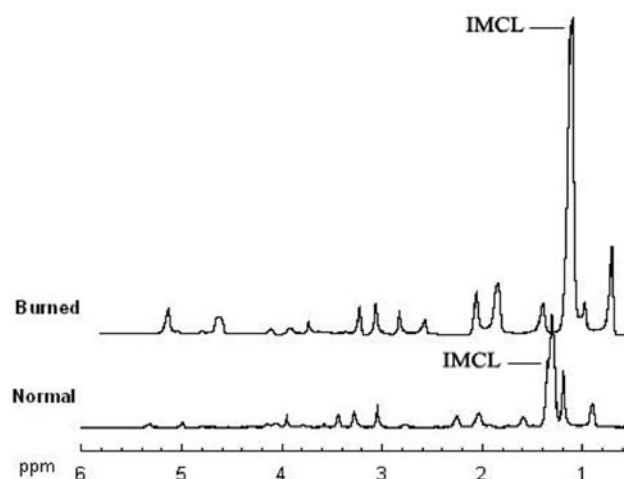


Figure 1. NMR spectra from  $^1\text{H}$ -NMR HRMAS experiments performed on the hind limb skeletal muscle specimens of mice. The spectra were acquired from normal and burned mice at 3 day post burn and were scaled to the phosphocreatine and creatine peak (3.02 ppm). The line indicates the position of IMCLs detected at 1.4 ppm. Resonance signals are due to residual water (4.7-4.8 ppm); terminal methyl (0.8-1.0 ppm); acyl chain methylene (1.1-1.5 ppm);  $\alpha$ - and  $\beta$ -methylene (2.0-2.5 ppm) and olefinic protons (5.4 ppm) of lipids; N-methyl protons of phosphocreatine and creatine (3.0 ppm); and N-trimethyl protons of betaines (3.2 ppm), which correspond to taurine and choline-containing compounds.

The tissue was postfixed and stained with 1% osmium tetroxide in 0.1 M cacodylate buffer, incubated with uranyl acetate, and dehydrated with ethanol. The tissues were subsequently rinsed with propylene oxide and embedded using Embed 812. Longitudinal and thin cross sections (60 nm) were counterstained with uranyl acetate and lead citrate and photographed on a Jeol 1200-Ex transmission electron microscope.

**Plasma FFA assay.** Blood was drawn by heart puncture at the time of sacrifice, and the plasma FFA level was measured by using the calorimetric FFA assay kit that uses acylation of coenzyme A (NEFA C; Wako Chemicals USA, Inc., Richmond, VA).

**Statistical analysis.** The Kolmogorov-Smirnov and Levene's tests were used to assess the normality of the variables and homogeneity of variances, respectively. Differences in ratios of IMCL levels (1.4 ppm) to total creatine (1.32 ppm) and  $T_2$  values between time groups were evaluated by using the non-parametric Kruskal-Wallis test. Analysis of variance (ANOVA) was also performed by using parametric and non-parametric methods to ensure that the differences or lack of differences between groups were consistent.

The Pearson product-moment correlation coefficient (R) was calculated to assess the correlation between the PGC-1 $\beta$  or IRS1 gene expression levels and levels of IMCLs or FFAs. Independent predictors of PGC-1 and IRS expression were analyzed with backward stepwise multiple linear regression with  $p < 0.05$  required for variables to be retained in the model. The coefficient of determination (adjusted  $R^2$ ) was used to measure model fit.

Statistical analysis was conducted using SPSS, version 12.0 (SPSS, Chicago, IL), and a two-tailed  $\alpha$  level of 0.05

Table I. Results of  $^1\text{H}$  NMR HRMAS experiments performed on hind limb skeletal muscle specimens from burned and normal mice.

	Normal (n=6)	6 h post burn (n=6)	24 h post burn (n=3)	72 h post burn (n=3)
IMCLs (a.u.)	0.8±0.1 <sup>a</sup>	2.4±0.3 p=0.007 <sup>b</sup>	8.3±1.1 p=0.024	9.1±0.8 p=0.007
T <sub>2</sub> (msec)	87±11	104±7 NS <sup>c</sup>	86±3 NS	96±13 NS

n, number of mice studied; IMCLs, intramyocellular lipids normalized to the creatine peak; T<sub>2</sub>, transverse relaxation time indicating non-significant mobility of IMCLs after burn; <sup>a</sup>values are the means ± standard errors; <sup>b</sup>p-values for comparisons between burned and normal mice obtained with the Games Howell test for IMCLs (the difference between 24 and 72 h was also significant; p=0.007); and <sup>c</sup>NS, non-significant difference between burned and normal mice obtained using the Tukeys test for T<sub>2</sub>.

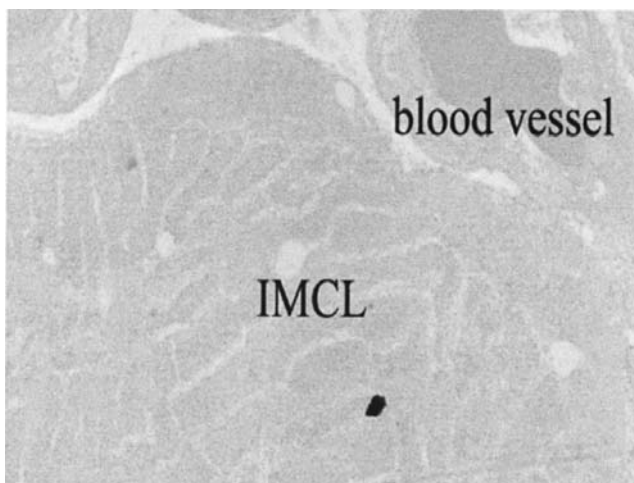


Figure 2. Electromicroscopy of burned muscle. IMCLs are shown as intracellular triglyceride stores.

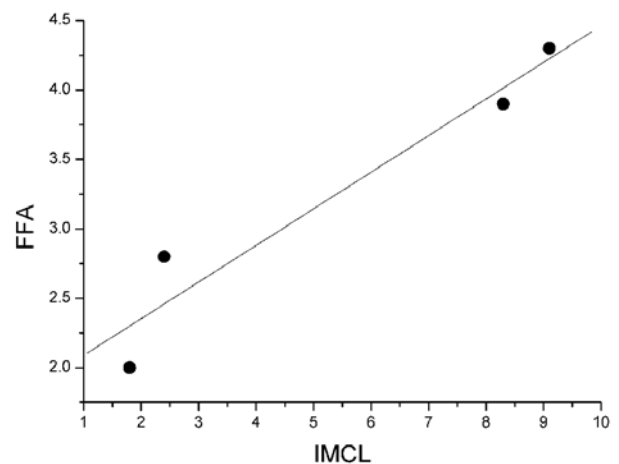


Figure 3. Correlation of plasma FFAs and intracellular triglyceride stores. An increase in the plasma FFA level post burn correlates significantly with IMCLs (or triglyceride stores). Pearson's correlation coefficient  $R=0.965$ ;  $p=0.035$ .

was used as the criterion for statistical significance for all comparisons.

## Results

*IMCLs as detected by NMR rise in proximal skeletal muscle and correlate significantly with the rise in plasma FFAs.* Fig. 1 shows representative  $^1\text{H}$ -NMR spectra acquired from normal and burned mice, and illustrates a notable post-burn rise in IMCLs. Quantitative results of these measurements (Table I) demonstrate a significant rise in ICMLs at 6, 24 and 72 h post burn. The T<sub>2</sub> of IMCLs did not change significantly with burn. Electron microscopy (EM) results also demonstrated that IMCLs accumulated post burn (Fig. 2). In addition, plasma levels of FFAs correlated significantly with IMCLs ( $R=0.965$ ;  $p=0.035$ ), as shown in Fig. 3.

*Burn injury downregulates the expression of Glut4, IRS1 and PGC-1 $\beta$ .* In our transcriptome studies, we compared the expression of all genes that might lead to metabolic dysfunction in skeletal muscle after burn. Here, we show the differential expression of certain metabolic genes at 3 time

points following a localized, but severe, hind limb burn (Table II). We observed downregulation of all of the genes shown post burn. IRS1 expression was downregulated at all 3 time points post burn; however, Glut4 expression was downregulated only at 72 h post burn. Finally, the expression of PGC-1 $\beta$  was downregulated at 6 h and reached a minimum at 24 h which was maintained at 72 h post burn.

*Plasma FFA level is a significant predictor of IRS1 and/or PGC-1 $\beta$  gene expression (Fig. 4).* Table III shows the results of our backward stepwise multiple linear regression and correlation analyses. FFA levels correlated with both IRS1 and PGC-1 $\beta$  expression, whereas the IMCL level correlated only with PGC-1 $\beta$ . The FFA level was a significant predictor of PGC-1 $\beta$  ( $p=0.097$ , adjusted  $R^2=0.723$ ) or IRS1 ( $p=0.038$ , adjusted  $R^2=0.887$ ) expression, but IMCL was not a significant predictor of either PGC-1 $\beta$  ( $p=0.562$ ) or IRS1 ( $p=0.468$ ) expression. Nevertheless, our correlation analysis showed that IMCL and FFA levels have a significant positive relationship (Fig. 3).

SPANDIDOS PUBLICATIONS Differential expression of metabolic genes at 6, 24 and 72 h post burn.

GenBank accession no.	Name of gene	Gene symbol	GO biological process	6 h	24 h	72 h
NM_009204	Solute carrier family 2 (facilitated glucose transporter), member 4	Slc2a4; Slc2a4; Glut4; Glut-4	Glucose transport	/	/	-2.15
NM_008063	Glucose-6-phosphatase, transport protein 1	G6pt1; G6pt1; GSD-1b	Glucose transport	/	/	-3.66
NM_008810	Pyruvate dehydrogenase E1 $\alpha$ 1	Pdha1; Pdha1; Pdha-1	Glycolysis	/	/	-1.89
AK011810	Pyruvate dehydrogenase (lipoamide) $\beta$	Pdhb; 2610103L06Rik	Glycolysis	/	/	-2.36
NM_133249	RIKEN cDNA 4631412G21; peroxisome proliferator-activated receptor $\gamma$ coactivator 1 $\beta$	4631412G21Rik; 4631412G21Rik; Perc	Lipid metabolism	-2.25	-2.91	-2.87
BB345784	Mus musculus cDNA clone B930058J01	Irs1		-2.06	-3.33	-3.38

Values are the relative expression intensity of the burn versus the control animals. Gene annotations for biological processes are from the Gene Ontology Consortium and the Ingenuity database. (/) not differentially expressed compared to the normal controls.

Table III. Correlations between plasma FFAs, IMCLs, and IRS1 and PGC-1 $\beta$  gene expression 6, 24 and 72 h post burn.

	IRS1	FFA	IMCL
Pearson correlation			
IRS1	-	-0.962	-0.874
FFA	-0.962	-	0.965
IMCL	-0.874	0.965	-
p-value			
IRS1	-	0.038	0.063
FFA	0.038	-	0.035
IMCL	0.063	0.035	-
-----			
	PGC-1 $\beta$	FFA	IMCL
Pearson correlation			
PGC-1 $\beta$	-	-0.903	-0.801
FFA	-0.903	-	0.965
IMCL	-0.801	0.965	-
p-value			
PGC-1 $\beta$	-	0.097	0.199
FFA	0.097	-	0.035
IMCL	0.199	0.035	-

FFA, plasma-free fatty acids; IRS1, insulin receptor substrate 1; IMCL, intramyocellular lipids by NMR; PGC-1 $\beta$ , peroxisome proliferator-activated receptor coactivator 1 (PPAR $\gamma$  coactivator-1 or PGC-1 $\beta$ ).

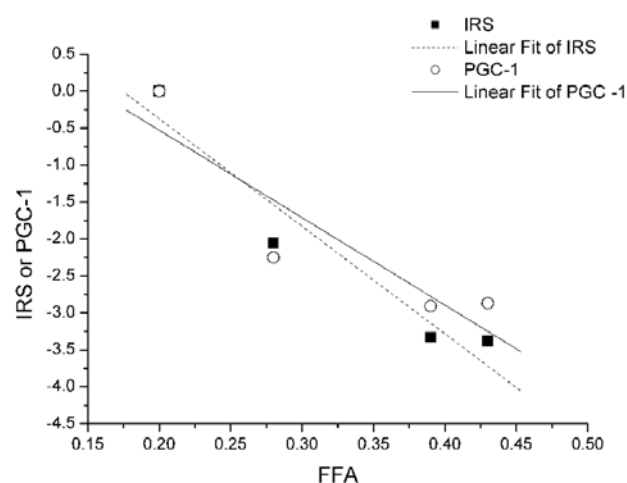


Figure 4. Correlation of plasma FFAs and IRS1 and PGC-1 $\beta$  gene expression. FFA levels correlate linearly with gene expression of both IRS1 (R= -0.962) and PGC-1 $\beta$  (R= -0.903).

## Discussion

The present study demonstrates that burn trauma results in: i) a significant increase of IMCLs or intracellular triglyceride stores in proximal skeletal muscle; ii) a rise in plasma FFAs; and iii) a downregulation of IRS1, Glut4 and PGC-1 $\beta$  mRNA levels. The downregulation of IRS1 and PGC-1 $\beta$  in skeletal muscle, which parallels the rise of plasma FFA levels, may be an upstream regulatory mechanism involving insulin resistance and mitochondrial uncoupling, leading to apoptosis

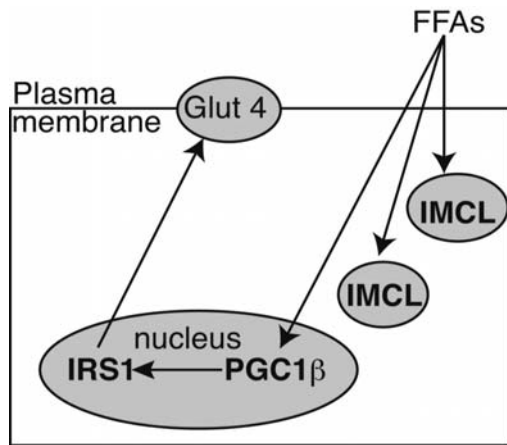


Figure 5. Proposed molecular mechanism of insulin resistance in skeletal muscle after burn. In this scheme, FFAs influence the accumulation of IMCLs and trigger PGC-1 $\beta$  which is an upstream regulator of IRS1. IRS1 in turn downregulates Glut4 and glucose transport, thus conferring insulin resistance in skeletal muscle. FFA, plasma-free fatty acids; IRS1, insulin receptor substrate 1; IMCL, intramyocellular lipid levels obtained by NMR; PGC-1 $\beta$ , peroxisome proliferator-activated receptor coactivator 1 (PPAR $\gamma$  coactivator-1) or PGC-1 $\beta$ .

as observed in burned skeletal muscle (4,26). Such a process may occur in response to the increased levels of reactive oxygen species (ROS) (11) and cytokines (i.e., TNF $\alpha$  observed in systemic burn) (3). Our findings suggest that IMCLs in skeletal muscle could serve as metabolic biomarkers related to inflammation, diabetes and obesity.

Here, we applied HRMAS  $^1\text{H}$  NMR to intact muscle samples from animals subjected to burn trauma in order to identify at high-resolution concomitant metabolic and molecular aberrations associated with insulin resistance and metabolic dysfunction. These changes might also reflect mitochondrial dysfunction, as some of the genes down-regulated in response to burn trauma encode mitochondrial-dependent metabolic functions (5). The strength of HRMAS is that it allows dual investigation of metabolic and molecular changes since the same specimens studied with HRMAS can subsequently be used for transcriptome studies (4). Compared with the use of conventional high-resolution *in vitro* NMR to examine tissue extracts exposed to burn trauma (27), *ex vivo* HRMAS NMR of intact tissue provides superior biochemical information, with simplified sample preparation and a better approximation of the *in vivo* state (4). To this end, this technique is increasingly being used to investigate overt cellular diseases (4,28-33).

In this, as well as in previous studies, increased IMCL levels are associated with insulin resistance (15), a major metabolic dysfunction that can develop as a result of severe burn trauma (3,6). The cytoplasmic localization of IMCLs as indicated by EM does not appear to change after severe burn, as indicated by a lack of change in ICML  $T_2$  levels post burn (Table II). Thus, these IMCLs or triglycerides are stored in the cytoplasm and appear to be metabolically inert, contributing to declining ATP synthesis (5). Previous measurements of muscle triglyceride content by biopsy (34) and IMCL content by  $^1\text{H}$  NMR spectroscopy (20,35) showed a strong relationship between intramuscular fat content and insulin resistance.

Although increased fatty acid delivery from lipolysis could also produce the observed IMCL increase, FFA concentrations are highly variable in burn patients (36). Also, impaired lipoprotein and polyunsaturated fatty acid metabolism occurs in the early post-burn period (37), suggesting their involvement in subsequent healing and immune responses. Previous genomic data alternatively suggest that the increased IMCL level could be the result of decreased mitochondrial oxidative capacity (5), in agreement with gene expression data in human diabetes (38). It has also been reported that increased IMCLs are associated with insulin resistance in type 2 diabetes (39), suggesting a role for IMCL levels in reducing mitochondrial oxidation and phosphorylation.

It has also been proposed that burn-induced insulin resistance may be related to the development of 'ectopic' fat stores. Triglyceride stores develop in sites such as the liver and muscle cells, due to increased FFA delivery following catecholamine-induced lipolysis, decreased  $\beta$ -oxidation within muscle, and decreased hepatic secretion of fats. These increases in intracellular triglyceride levels may contribute to the observed alterations in insulin signaling (40). In accordance with this, the IMCL accumulation detected by NMR in this study qualifies as a biomarker of altered insulin resistance and signaling in burn trauma.

One major finding of our experiments is that a rise in IMCLs correlates positively with plasma FFAs, which also rise in many insulin-resistant states, including not only burn trauma but also type 2 diabetes and obesity (41-43). FFAs are also a significant predictor of IRS1 and PGC-1 $\beta$  gene expression. Our results corroborate what has been previously reported for insulin resistance in human skeletal muscle, that is, that increased plasma FFAs induce insulin resistance through inhibition of glucose transport activity, which may be a consequence of decreased IRS1 activity (43). Based on our study, the expression profile of the IRS1 insulin substrate, which was significantly reduced by 6 h post burn and continued to decrease thereafter, may suggest that FFAs affect IRS1 expression, which in turn affects Glut4 expression and glucose transport by 72 h post burn. This observed decrease in glucose transport is in agreement with several previous studies (44-47), including a study performed in rats where alterations in post-receptor insulin signaling were implicated as one mechanism for post-burn insulin resistance (3). We found that the expression of PGC-1 $\beta$  was also affected by burn (Table II). Although our results do not indicate whether IRS1 expression affects PGC-1 $\beta$  or vice versa, because PGC-1 $\beta$  is a transcriptional co-activator, we postulate that it acts as an upstream regulator of metabolic genes, including IRS1 (11). If this is so, then PGC-1 $\beta$  may also contribute to burn-induced insulin resistance. It may be, that in burn, ROS affect PGC-1 $\beta$  which affects a myriad of other genes important in metabolism and insulin resistance. Although further studies are needed to examine this hypothesis, nevertheless, our present study strongly implicates IMCLs as metabolic biomarkers of glucose homeostasis and fatty acid metabolism in pathological states such as burn.

The transcriptome findings presented here suggest that burn trauma results in reduced IRS1 and PGC-1 $\beta$  gene expression by skeletal muscle nuclei. This was validated by NMR spectroscopy, which uncovered increased IMCLs or



SPANDIDOS  
PUBLICATIONS

de stores in the post-burn skeletal muscle cytoplasm. Results can be explained by the downregulation of genes involved in  $\beta$ -oxidation and an absence of ATP synthesis, which lead to the mitochondrial dysfunction that underlies skeletal muscle wasting and the general cachexia of burn pathophysiology (5). It has been shown that PGC-1 $\beta$  (like PGC1- $\alpha$ ) increases mitochondrial biogenesis and respiration when expressed in muscle cells, implicating a role for this gene in mitochondrial metabolism (48). Recently, PGC-1 $\beta$  was also recognized as an activator of uncoupling proteins, which greatly reduce mitochondrial ROS production (13). Thus, we propose that the downregulation of PGC-1 $\beta$  observed in this study leaves the muscle unprotected against the harmful oxidative damage of ROS, which is probably exacerbated by burn. Combining these various results, we propose a potential molecular mechanism for burn-induced skeletal muscle insulin resistance (Fig. 5).

Finally, we believe that our findings may be clinically relevant in molecular medicine, since a) both FFAs and IMCLs can be measured clinically using non-invasive and non-irradiating procedures; b) the activity of PGC-1 $\beta$  may be induced; and c) PGC-1 $\beta$  agonists may alleviate post-burn insulin resistance (49) and prevent burn-induced damage in remote organs (50). These findings open the door to a better understanding of molecular and metabolic processes attendant to local burn trauma and/or other traumatic situations.

### Acknowledgements

This work was supported in part by a Shriners Hospital for Children Research Grant no. 8893 to A. Aria Tzika, by a National Institutes of Health (NIH) Center Grant no. P50GM021700 to Ronald G. Tompkins, and by a Center Grant of the National Institutes of Health to the Stanford Genome Technology Center. Qunhao Zhang was a Shriners Research Fellow. We thank Dr David Zurakowski for reviewing the statistical analysis. We also thank Dr Katie Edmondson and Dr Ann Power Smith of Write Science Right for the editorial assistance.

### References

- Meislin H, Criss EA, Judkins D, *et al*: Fatal trauma: the modal distribution of time to death is a function of patient demographics and regional resources. *J Trauma* 43: 433-440, 1997.
- Meel BL: Incidence and patterns of violent and/or traumatic deaths between 1993 and 1999 in the Transkei region of South Africa. *J Trauma* 57: 125-129, 2004.
- Ikezu T, Okamoto T, Yonezawa K, Tompkins RG and Martyn JA: Analysis of thermal injury-induced insulin resistance in rodents. Implication of postreceptor mechanisms. *J Biol Chem* 272: 25289-25295, 1997.
- Astrakas LG, Goljer I, Yasuhara S, *et al*: Proton NMR spectroscopy shows lipids accumulate in skeletal muscle in response to burn trauma-induced apoptosis. *FASEB J* 19: 1431-1440, 2005.
- Padfield KE, Astrakas LG, Zhang Q, *et al*: Burn injury causes mitochondrial dysfunction in skeletal muscle. *Proc Natl Acad Sci USA* 102: 5368-5373, 2005.
- Muller MJ and Herndon DN: The challenge of burns. *Lancet* 343: 216-220, 1994.
- Deitch EA: The management of burns. *N Engl J Med* 323: 1249-1253, 1990.
- Roden M, Price TB, Perseghin G, *et al*: Mechanism of free fatty acid-induced insulin resistance in humans. *J Clin Invest* 97: 2859-2865, 1996.
- McGarry JD: Banting lecture 2001: dysregulation of fatty acid metabolism in the etiology of type 2 diabetes. *Diabetes* 51: 7-18, 2002.
- Spiegelman BM and Heinrich R: Biological control through regulated transcriptional coactivators. *Cell* 119: 157-167, 2004.
- Handschin C and Spiegelman BM: Peroxisome proliferator-activated receptor gamma coactivator 1 coactivators, energy homeostasis, and metabolism. *Endocr Rev* 27: 728-735, 2006.
- Kressler D, Schreiber SN, Knutti D and Kralli A: The PGC-1-related protein PERC is a selective coactivator of estrogen receptor alpha. *J Biol Chem* 277: 13918-13925, 2002.
- Lin J, Handschin C and Spiegelman BM: Metabolic control through the PGC-1 family of transcription coactivators. *Cell Metab* 1: 361-370, 2005.
- Szczepaniak LS, Babcock EE, Schick F, *et al*: Measurement of intracellular triglyceride stores by H spectroscopy: validation in vivo. *Am J Physiol* 276: E977-E989, 1999.
- Kuhlmann J, Neumann-Haefelin C, Belz U, Kramer W, Juretschke HP and Herling AW: Correlation between insulin resistance and intramyocellular lipid levels in rats. *Magn Reson Med* 53: 1275-1282, 2005.
- Boesch C, Slotboom J, Hoppeler H and Kreis R: In vivo determination of intra-myocellular lipids in human muscle by means of localized 1H-MR-spectroscopy. *Magn Reson Med* 37: 484-493, 1997.
- Schick F, Eismann B, Jung WI, Bongers H, Bunse M and Lutz O: Comparison of localized proton NMR signals of skeletal muscle and fat tissue in vivo: two lipid compartments in muscle tissue. *Magn Reson Med* 29: 158-167, 1993.
- Neumann-Haefelin C, Kuhlmann J, Belz U, *et al*: Determinants of intramyocellular lipid concentrations in rat hindleg muscle. *Magn Reson Med* 50: 242-248, 2003.
- Hwang JH, Pan JW, Heydari S, Hetherington HP and Stein DT: Regional differences in intramyocellular lipids in humans observed by in vivo 1H-MR spectroscopic imaging. *J Appl Physiol* 90: 1267-1274, 2001.
- Krissak M, Petersen KF, Dresner A, *et al*: Intramyocellular lipid concentrations are correlated with insulin sensitivity in humans: a 1H NMR spectroscopy study. *Diabetologia* 42: 113-116, 1999.
- Jacob S, Machann J, Rett K, *et al*: Association of increased intramyocellular lipid content with insulin resistance in lean nondiabetic offspring of type 2 diabetic subjects. *Diabetes* 48: 1113-1119, 1999.
- Goodpaster BH, He J, Watkins S and Kelley DE: Skeletal muscle lipid content and insulin resistance: evidence for a paradox in endurance-trained athletes. *J Clin Endocrinol Metab* 86: 5755-5761, 2001.
- Anderwald C, Bernroider E, Krissak M, *et al*: Effects of insulin treatment in type 2 diabetic patients on intracellular lipid content in liver and skeletal muscle. *Diabetes* 51: 3025-3032, 2002.
- Sinha R, Dufour S, Petersen KF, *et al*: Assessment of skeletal muscle triglyceride content by (1)H nuclear magnetic resonance spectroscopy in lean and obese adolescents: relationships to insulin sensitivity, total body fat, and central adiposity. *Diabetes* 51: 1022-1027, 2002.
- Tomera JF and Martyn J: Systemic effects of single hindlimb burn injury on skeletal muscle function and cyclic nucleotide levels in the murine model. *Burns Incl Therm Inj* 14: 210-219, 1988.
- Yasuhara S, Perez ME, Kanakubo E, *et al*: Skeletal muscle apoptosis after burns is associated with activation of proapoptotic signals. *Am J Physiol Endocrinol Metab* 279: E1114-E1121, 2000.
- Lee K, Berthiaume F, Stephanopoulos GN, Yarmush DM and Yarmush ML: Metabolic flux analysis of postburn hepatic hypermetabolism. *Metab Eng* 2: 312-327, 2000.
- Morvan D, Demidem A, Papon J, De Latour M and Madelmont JC: Melanoma tumors acquire a new phospholipid metabolism phenotype under cysteamine as revealed by high-resolution magic angle spinning proton nuclear magnetic resonance spectroscopy of intact tumor samples. *Cancer Res* 62: 1890-1897, 2002.
- Tzika AA, Cheng LL, Goumnerova L, *et al*: Biochemical characterization of pediatric brain tumors by using in vivo and ex vivo magnetic resonance spectroscopy. *J Neurosurg* 96: 1023-1031, 2002.

30. Griffin JL, Lehtimäki KK, Valonen PK, *et al*: Assignment of <sup>1</sup>H nuclear magnetic resonance visible polyunsaturated fatty acids in BT4C gliomas undergoing ganciclovir-thymidine kinase gene therapy-induced programmed cell death. *Cancer Res* 63: 3195-3201, 2003.
31. Griffin JL and Shockcor JP: Metabolic profiles of cancer cells. *Nat Rev Cancer* 4: 551-561, 2004.
32. Griffin JL and Kauppinen RA: A metabolomics perspective of human brain tumours. *FEBS J* 274: 1132-1139, 2007.
33. Tzika AA, Astrakas L, Cao H, *et al*: Combination of high-resolution magic angle spinning proton magnetic resonance spectroscopy and microscale genomics to type brain tumor biopsies. *Int J Mol Med* 20: 199-208, 2007.
34. Johnson AB, Argyraki M, Thow JC, Cooper BG, Fulcher G and Taylor R: Effect of increased free fatty acid supply on glucose metabolism and skeletal muscle glycogen synthase activity in normal man. *Clin Sci* 82: 219-226, 1992.
35. Perseghin G, Scifo P, De Cobelli F, *et al*: Intramyocellular triglyceride content is a determinant of in vivo insulin resistance in humans: a <sup>1</sup>H-<sup>13</sup>C nuclear magnetic resonance spectroscopy assessment in offspring of type 2 diabetic parents. *Diabetes* 48: 1600-1606, 1999.
36. Galster AD, Bier DM, Cryer PE and Monafo WW: Plasma palmitate turnover in subjects with thermal injury. *J Trauma* 24: 938-945, 1984.
37. Pratt VC, Tredget EE, Clandinin MT and Field CJ: Fatty acid content of plasma lipids and erythrocyte phospholipids are altered following burn injury. *Lipids* 36: 675-682, 2001.
38. Mootha VK, Lindgren CM, Eriksson KF, *et al*: PGC-1 $\alpha$ -responsive genes involved in oxidative phosphorylation are coordinately downregulated in human diabetes. *Nat Genet* 34: 267-273, 2003.
39. Petersen KF, Dufour S, Befroy D, Garcia R and Shulman GI: Impaired mitochondrial activity in the insulin-resistant offspring of patients with type 2 diabetes. *N Engl J Med* 350: 664-671, 2004.
40. Cree MG and Wolfe RR: Post burn trauma insulin resistance and fat metabolism. *Am J Physiol Endocrinol Metab* 294: E1-E9, 2008.
41. Steiner G, Morita S and Vranic M: Resistance to insulin but not to glucagon in lean human hypertriglyceridemics. *Diabetes* 29: 899-905, 1980.
42. Reaven GM, Hollenbeck C, Jeng CY, Wu MS and Chen YD: Measurement of plasma glucose, free fatty acid, lactate, and insulin for 24 h in patients with NIDDM. *Diabetes* 37: 1020-1024, 1988.
43. Dresner A, Laurent D, Marcucci M, *et al*: Effects of free fatty acids on glucose transport and IRS-1-associated phosphatidylinositol 3-kinase activity. *J Clin Invest* 103: 253-259, 1999.
44. Le Marchand-Brustel Y, Jeanrenaud B and Freychet P: Insulin binding and effects in isolated soleus muscle of lean and obese mice. *Am J Physiol* 234: E348-E358, 1978.
45. Molloy RG, O'Riordain M, Holzheimer R, *et al*: Mechanism of increased tumor necrosis factor production after thermal injury. Altered sensitivity to PGE<sub>2</sub> and immunomodulation with indomethacin. *J Immunol* 151: 2142-2149, 1993.
46. Yonezawa K, Ando A, Kaburagi Y, *et al*: Signal transduction pathways from insulin receptors to Ras. Analysis by mutant insulin receptors. *J Biol Chem* 269: 4634-4640, 1994.
47. Hotamisligil GS, Peraldi P, Budavari A, Ellis R, White MF and Spiegelman BM: IRS-1-mediated inhibition of insulin receptor tyrosine kinase activity in TNF- $\alpha$ - and obesity-induced insulin resistance. *Science* 271: 665-668, 1996.
48. St-Pierre J, Lin J, Krauss S, *et al*: Bioenergetic analysis of peroxisome proliferator-activated receptor gamma coactivators 1 $\alpha$  and 1 $\beta$  (PGC-1 $\alpha$  and PGC-1 $\beta$ ) in muscle cells. *J Biol Chem* 278: 26597-26603, 2003.
49. Cree MG, Zwetsloot JJ, Herndon DN, *et al*: Insulin sensitivity and mitochondrial function are improved in children with burn injury during a randomized controlled trial of fenofibrate. *Ann Surg* 245: 214-221, 2007.
50. Sener G, Sehirli AO, Gedik N and Dulger GA: Rosiglitazone, a PPAR- $\gamma$  ligand, protects against burn-induced oxidative injury of remote organs. *Burns* 33: 587-593, 2007.